Role of FBXL19-AS1 in hepatocellular carcinoma by lncRNA–miRNA–mRNA network analysis and its diagnostic and prognostic value

Dingdong He
Wuhan University Zhongnan Hospital
Xiaokang Zhang
Wuhan University Zhongnan Hospital
Xinyu Zhu
Wuhan University Zhongnan Hospital
Narayani Maharjan
Wuhan University Zhongnan Hospital
Yingchao Wang
Wuhan University Zhongnan Hospital
Ping Luo
Wuhan University Zhongnan Hospital
Chunzi Liang
Wuhan University Zhongnan Hospital
Jiancheng Tu (jianchengtu@whu.edu.cn)
Wuhan University Zhongnan Hospital https://orcid.org/0000-0003-4304-1593

Research

Keywords: FBXL19-AS1, hepatocellular carcinoma, biomarker, pathogenesis, ceRNA

Posted Date: July 23rd, 2020

DOI: https://doi.org/10.21203/rs.3.rs-44069/v1

Abstract

Background: Hepatocellular carcinoma (HCC) is one of the most common neoplastic diseases worldwide. Available biomarkers are not sensitive enough for the diagnosis of HCC, seeking new biomarkers of HCC is urgent and challenging. The purpose of this study was to investigate the role of F-box and leucine-rich repeat protein 19-antisense RNA 1 (FBXL19-AS1) through competing endogenous RNA (ceRNA) network and its diagnostic and prognostic value in HCC.

Methods: A comprehensive strategy of genomic data mining, bioinformatics and experimental validation was used to evaluate the clinical value of FBXL19-AS1 in the diagnosis and prognosis of HCC and to identify the pathways that FBXL19-AS1 may be involved in.

Results: FBXL19-AS1 was up-regulated in HCC, and its high expression was associated with TNM stage and poor prognosis of HCC patients. The combined use of plasma FBXL19-AS1 and alpha-fetoprotein (AFP) could prominently improve the diagnostic validity for HCC. FBXL19-AS1 might participate in regulating HCC related pathways, including hepatitis C, hepatitis B, microRNAs in cancer, cell cycle, viral carcinogenesis, and proteoglycans in cancer through ceRNA network.

Conclusions: Our findings indicated that FBXL19-AS1 not only serves as a potential biomarker for HCC diagnosis and prognosis, but it may be functionally carcinogenic.

Background

Liver cancer is a common malignant cancer globally. According to the latest global cancer statistics, liver cancer ranks sixth and fourth in morbidity and mortality among all types of cancers, respectively [1]. Hepatocellular carcinoma (HCC) accounts for 70%-85% of primary liver cancers, is the most common form of liver cancer. Recent years have witnessed a great gain in treatment methods of HCC, such as surgical resection, liver transplantation, adjuvant therapy, interventional therapy and so on. [2–3]. The 5-year survival rate of HCC patients with early diagnosis and appropriate treatment or intervention is more than 50% [4], but for those who are diagnosed and treated after the relevant symptoms appear, the 5-year survival rate is only 14.1% [5]. Currently, although alpha-fetoprotein (AFP) has been reported to be a valid marker for the clinical diagnosis and prognosis of HCC, its value remains unsatisfied in early diagnosis. To improve the outcome and prognosis of HCC patients, it's essential to find more effective biomarkers to improve the early diagnosis of HCC [6].

Studies have found that non-coding RNAs (ncRNAs) such as microRNAs (miRNAs) and long non-coding RNAs (lncRNAs) are involved in regulating proliferation, invasion and metastasis of HCC cells, providing a novel perspective for the diagnosis and prognosis of HCC [7]. The competitive endogenous RNA (ceRNA) mechanism is one of the classical mechanisms for the regulation of ncRNAs. Salmena et al first proposed the ceRNA hypothesis that ceRNAs can bind to miRNAs via miRNA response elements (MREs), thereby affecting miRNA-induced gene silencing and playing an important role in pathological conditions

such as cancer [8]. FBXL19-AS1, a lncRNA functions as a ceRNA was widely documented in various cancer studies except for HCC [9–14].

In the present study, The Cancer Genome Atlas liver hepatocellular carcinoma (TCGA LIHC) dataset [15] and 6 HCC related microarrays from Gene Expression Omnibus (GEO) database [16] were analyzed combinedly to obtain differentially expressed lncRNAs in HCC tissues. FBXL19-AS1 was filtered to be up-regulated in HCC and was predicted to predominantly exist in the cytosol by the LncLocator database [17]. In addition, it was found enriched in inflammation and cancer-related pathways through Gene Set Enrichment Analysis (GSEA). Therefore, our study constructed a rigorous ceRNA network involved in FBXL19-AS1 and demonstrated the possible significant value of FBXL19-AS1 in the early diagnosis and prognosis of HCC.

Methods

Data source

A part of datasets was obtained from GEO database. We performed comprehensive retrieve on the publicly available HCC non-coding RNA datasets from GEO database (https://www.ncbi.nlm.nih.gov/geo/). Datasets were included in this study based on the following inclusion criteria: (1) datasets contained both normal and HCC samples; (2) HCC subjects were pathologically diagnosed based on clinical and histopathological criteria and without limitation on the clinicopathological stage; (3) type of datasets was non-coding RNA profiling by array; (4) datasets contained more than 5000 lncRNAs. Based on the criteria above, we downloaded 6 HCC datasets from GEO database, including GSE58043, GSE67260, GSE112613, GSE89186, GSE64631 and GSE70880. In consideration of the limited sample size of single dataset could lead to unreliable results and reduce the effectiveness of bioinformatics analysis, we first integrated all samples of 6 datasets to significantly increase the sample size (39 normal samples vs 44 HCC samples). Heterogeneity and potential variables are generally recognized as the main sources of bias and variability in high-throughput experiments. The merged data was preprocessed by SVA [18] with R software (Version 3.5.3) to remove the batch effect and heterogeneity among virous datasets. If a gene corresponded to multiple probes, we took the average as its expression value. Differentially expressed lncRNAs were screened out using the limma package [19] in R software and the threshold was $|\log_2(\text{foldchange})| > 1$, adjust P value < 0.05.

The other part of data was from TCGA LIHC dataset (https://portal.gdc.cancer.gov/), which contained 50 normal samples and 374 tumor samples. Differentially expressed lncRNAs were filtered using the edgeR package [20] in R software and the threshold was $|\log_2(\text{foldchange})| > 1$, adjust P value < 0.05. An additional file shows details of each dataset [see Additional file 1].

GSEA

GSEA is a bioinformatics method that inspects the statistical significance of a priori defined set of genes and verifies the differences between two biological states [21]. Samples from TCGA were divided into 2

subgroups on the basis of the median expression of FBXL19-AS1. Genes from each sample were ranked according to the expression difference between the 2 subgroups by GSEA software 4.0. KEGG gene set was analyzed to explore pathways enriched in each subgroup. Gene set permutations were executed for 1000 times in the analysis. Normalized *P* value < 0.05 was taken as the threshold.

Tissue and Plasma Samples

Surgical specimens were obtained from 57 HCC patients (52 males and 5 females) in Zhongnan Hospital of Wuhan University (Wuhan, China) from 2015 to 2019. None of the patients received preoperative chemotherapy or radiotherapy. The follow-up period ranged from 2 months to 48 months. Whole blood samples were collected during 2017 and 2019 from Zhongnan Hospital of Wuhan University, which contained 79 healthy people, 77 patients with hepatitis B, 80 patients with cirrhosis, and 92 patients with HCC. All whole blood samples were collected into the EDTA anticoagulant tubes and the plasma was isolated at 12000 g for 5min in 4℃. Tissue and plasma samples were stored at -80℃ until use. All patients were diagnosed based on their pathological reports. The tumor stages were identified according to the seventh edition of the American Joint Committee on Cancer (AJCC) Cancer Staging Manual. The detailed clinicopathological information of all patients was shown in Table 1 and Table 2. All experimental schemes were approved by the Ethics Committee of Zhongnan Hospital of Wuhan University.

RNA extraction and quantitative real-time PCR

Total RNA was isolated from tissues by TRIZOL reagent (Invitrogen, USA), and RNA from plasm was extracted by RNA Separate Extraction Kit (Bioteke, China). NanoDrop 2000C (Thermo Fisher Scientific, USA) was applied to evaluate the concentration and purity of extracted RNA. Then ReverTra Ace qPCR RT Master Mix with gDNA Remover (Toyobo, Japan) was used to reversely transcribed RNA into complementary DNA (cDNA) at 37℃ for 15min, 50℃ for 5min and 98℃ for 5min. The quantitative real-time PCR (qPCR) was carried out using SYBR Green I UltraSYBR Mixture (CWBIO, China) on Bio-Rad CFX96 (Bio-Rad Laboratories, USA). We took *glyceraldehyde 3-phosphate dehydrogenase (GAPDH)* as endogenous reference gene to normalize the expression level among multiple samples. The specific sequences of each pair of primers were available in an additional file shows [see Additional file 2]. Relative gene expression status was calculated by $2^{-\Delta Cq}$. All experiments were repeated twice to intensify the credibility.

Survival analysis

Gene Expression Profiling Interactive Analysis2 (GEPIA2, http://gepia2.cancer-pku.cn/) is an online tool for gene expression and survival analysis based on tumor and normal samples from TCGA and GTEx Databases [22]. Overall survival was evaluated with the Kaplan-Meier method and compared by the log-rank test on GEPIA2. We set the dataset as LIHC and retrieved the overall survival of FBXL19-AS1 to obtain the information on the relationship between FBXL19-AS1 expression and prognosis of HCC. To

further verify the results, 57 HCC patients from Zhongnan Hospital of Wuhan University were followed up and survival analysis was performed on the basis of FBXL19-AS1 expression status.

Prediction of miRNAs

MiRcode V11 (http://www.mircode.org/) was used for prediction miRNA which would interact with FBXL19-AS1. The highly conserved microRNA families file was downloaded from the miRcode V11 website, and R software was used to predict the complementary miRNAs of FBXL19-AS1. Simultaneously, edgeR package in R software was used to screen out the differentially expressed miRNAs ($p<0.05$) in HCC based on TCGA. Then we took the intersection of the 2 miRNA lists so as to screened out miRNAs that were both interacted with FBXL19-AS1 and differentially expressed in HCC.

MiRNA expression verification

In order to further enhance the credibility of the differential expression of the predicted target miRNAs in HCC, we retrieved studies that contained miRNA expression data from TCGA and GEO for verification. All studies included both HCC and normal samples and the sample size of each subgroup was no less than 3. Data were extracted from each study as follows: first author, year of publication, region, data source, platform, miRNA ID, number of cases, and miRNA expression level. Combined standard mean difference (SMD) and 95% confidence interval (95% CI) were calculated by STATA 15.0 (STATA Corp, USA). Compared with the normal control, SMD > 0 indicates miRNA is up-regulated in HCC samples, while SMD < 0 indicates miRNA is down-regulated in HCC samples. Statistically significant threshold of two-sided *P* value was set at 0.05.

MiRNA targets prediction

To ensure the miRNA-mRNA interactions conserved in essential cancer pathways, target genes of miRNAs supported simultaneously by miRDB, miRTarBase, and TargetScan were selected by R software. Meanwhile, edgeR package in R software was used to screen out the differentially expressed mRNAs ($p<0.05$) in HCC based on TCGA. In addition, genes co-expressed with FBXL19-AS1 were obtained from cBioPortal database ($P < 0.05$). Finally, the intersection of the 3 lists was taken as the final target mRNAs.

Establishment of lncRNA-miRNA-mRNA expression network

We constructed a ceRNA network for FBXL19-AS1, target miRNAs and mRNAs. Cytoscape 3.7.2 software was used to visualize the network.

PPI network construction and hub genes selection

Analysis of PPI network is helpful in systematically studying the molecular mechanism of diseases and finding new drug targets. In our study, STRING (V11.0) (https://string-db.org/) [23] was adopted to establish a PPI network, and 0.4 was used as the threshold for interaction score. Subsequently, 12 kinds of algorithms (MCC, DMNC, MNC, Degree, EPC, BottleNeck, EcCentricity, Closeness, Radiality,

Betweenness, Stress, ClusteringCoefficient) were jointly used to identify hub genes through Cytoscape 3.7.2 software [24]. We took genes whose sum algorithm scores were more than 10000 to construct hub gene network.

Functional enrichment analysis of hub genes

R software and clusterProfiler package [25] were used to execute the Gene Ontology (GO) and Kyoto Encyclopedia of Genes and Genomes (KEGG) enrichment analysis [26,27]. Subsequently, the ggplot2 package was used to visualize the results, and the cut-off value of statistical significance was set to $P < 0.05$.

Statistical analysis

All statistical analyses of this research were conducted through SPSS version 25.0 (SPSS Inc., USA) and GraphPad Prism 8.0 (GraphPad Inc., USA). Mean ± standard deviation (SD) was used to describe the continuous variables of normal distribution. Median and quartile was used to describe the continuous variable of skewed distribution. The paired sample t test or Kruskal-Wallis test were utilized to compare the differences between the two groups. The chi-square test or Fisher exact test were used to compare the categorical variables between groups. Correlation analysis was performed by Pearson or Spearman test. Receiver operation curve (ROC) was used to evaluate the diagnostic value. The best cutoff point for sensitivity and specificity was selected by using the Jorden index. Overall survival was evaluated by Kaplan-Meier method and compared by log-rank test. The cutoff value of statistical significance was set as $P < 0.05$.

Results

The long noncoding RNA expression profile of HCC

The research flow diagram of this study was shown in Fig. 1. To identify lncRNAs that were differentially expressed in HCC, 6 GEO datasets were integrated into analysis (39 normal samples vs 44 HCC samples), including GSE58043, GSE67260, GSE112613, GSE89186, GSE64631 and GSE70880. We obtained 66 differentially expressed lncRNAs, among which 37 were up-regulated and 29 were down-regulated (Fig. 2a). Then we downloaded the relevant expression profiles of the TCGA LIHC dataset (50 normal samples vs 374 HCC samples) and obtained 2685 differentially expressed lncRNAs, among which 2323 were up-regulated and 362 were down-regulated (Fig. 2b). There were 26 lncRNAs that both differentially expressed in GEO joint dataset and TCGA LIHC dataset, among which 15 were up-regulated and 11 were down-regulated (Fig. 2c). An additional file shows these in more detail [see Additional file 3]. The expression heatmaps of GEO joint dataset and TCGA LIHC were displayed in Fig. 2d and Fig. 2e, respectively.

The potential interactive miRNAs of 26 differentially expressed lncRNAs were screened by R software based on the highly conserved microRNA families file downloaded from the miRcode V11 database. R

software predicted the target genes of corresponding miRNAs that were simultaneously supported in miRDB, miRTarBase and TargetScan. Only 7 lncRNAs (LINC00221, FAM99B, LINC00355, MAGI2-AS3, CRNDE, PWRN1, FBXL19-AS1) were predicted to have highly conserved targeted miRNAs [see Additional file 4]. We used GEPIA2 to carry out survival analyses for these 7 lncRNAs, and found that only FBXL19-AS1 (Fig. 3a), FAM99B (Fig. 3b) and CRNDE (Fig. 3c) were associated with the prognosis of HCC patients. Among the 3 lncRNAs, the function of FBXL19-AS1 in HCC has not yet been studied and FBXL19-AS1 might serve as a novel HCC biomarker. Therefore, FBXL19-AS1 was selected for further study.

FBXL19-AS1 was significantly up-regulated in both GEO joint dataset and TCGA LIHC datasets and mainly enriched on cell cycle, cancer and inflammation-related pathways by GSEA (Fig. 3d). We speculated that FBXL19-AS1 might play an important role in the occurrence, development and prognosis of HCC. In addition, we found that FBXL19-AS1 was located in cytosol according to the LncLocator database [see Additional file 5], which was the basis of establishing a more reliable ceRNA network. Interestingly, FBXL19, the complementary gene of FBXL19-AS1, was found to be positively correlated with the tumor infiltrating immune cells (TIICs) in HCC, including B cells, CD8+ T cells, CD4+ T cells, macrophages, neutrophils and dendritic cells [see Additional file 6].

Expression of FBXL19-AS1 in HCC tissues and its prognostic value

In order to verify the expression status of FBXL19-AS1 in HCC patients and to study its clinical significance, we collected 57 pairs of fresh tissues including HCC and adjacent non-tumor tissues. The qPCR results showed that the expression of FBXL19-AS1 in HCC tissue was significantly higher than adjacent non-tumor tissue (Fig. 4a).

The results on the study of the correlation between FBXL19-AS1 expression and clinicopathological features showed in Table1 that the over expression of FBXL19-AS1 was significantly correlated with higher GGT ($P = 0.046$), higher AFP ($P = 0.020$) and worse TNM stage ($P = 0.043$), which was consistent with what we predicted in GEPIA2 [see Additional file 4].

To further verify the prognostic value of FBXL19-AS1 in HCC, we performed Kaplan-Meier survival analysis and log-rank test in 57 HCC patients with intact prognostic information. The results showed that HCC patients with elevated FBXL19-AS1 had shorter overall survival ($P = 0.030$) (Fig. 4b), hinting FBXL19-AS1 might be an important prognostic factor for HCC.

Expression of FBXL19-AS1 in plasma and its diagnostic value

FBXL19-AS1 expression level was also checked through qPCR in plasma samples, which were taken from 79 healthy subjects, 77 patients with hepatitis B, 80 patients with cirrhosis, and 92 patients with HCC (Fig. 4c). The results showed that the expression of FBXL19-AS1 in plasma was significantly higher in hepatitis B, cirrhosis, and HCC patients than in healthy subjects ($P < 0.001$). While the expression of FBXL19-AS1 in HCC patients was higher than that of hepatitis B patients ($P = 0.016$) and cirrhosis patients ($P = 0.004$). The main clinical features of the plasma samples were shown in Table 2. From

which the expression of FBXL19-AS1 in each group was correlated with the plasma alanine aminotransferase (ALT) ($P < 0.001$), aspartate aminotransferase (AST) ($P < 0.001$), albumin (ALB) ($P < 0.001$), alpha fetoprotein (AFP) ($P < 0.001$), but not with gender, age, CEA or other biochemical indicators.

ROCs of FBXL19-AS1 in HCC, drawn to evaluate the diagnostic value, indicated FBXL19-AS1 was with moderate diagnostic ability to distinguish HCC patients from healthy people (AUC = 0.875, $P < 0.001$). Intergation of AFP, the most commonly detected biomarker for the diagnosis of HCC whose predictive value alone was rather low (AUC = 0.769, $P < 0.001$), with FBXL19-AS1, its preditive validity was significantly improved (AUC = 0.931, $P < 0.001$). (Table3, Fig. 4d-i).

78 miRNAs were obtained as the potential target miRNAs of FBXL19-AS1 through binding site search from miRcode V11 database. 24 miRNAs were selected after comparing with the 467 differentially expressed miRNAs screened from TCGA ($P < 0.05$). Subsequently, miRNA target genes were predicted and only 7 of the above 24 miRNAs met our requirements (has-miR-142-3p, hsa-miR-125a-5p, hsa-miR-216b-5p, hsa-miR-107, hsa-miR-17-5p, has-miR-20b-5p, has-miR-22-3p). Afterwards, we explored signaling pathways related with the 7 miRNAs through DIANA-miRPath. As shown in Fig. 5, the 7 miRNAs were essentially involved in the initiation and progression of many types of cancers. Among them, pathways that might be related to HCC were mTOR signaling pathway, Hedgehog signaling pathway, hepatitis B, hepatitis C, p53 signaling pathway, Wnt signaling pathway, GnRH signaling pathway, ErbB signaling pathway, PI3K-Akt signaling pathway, MAPK signaling pathway, etc.

Validation of miRNA expression based on GEO and TCGA database

To evaluate the expression of these 7 miRNAs in HCC, 9 GSE microarrays from GEO and dataset from TCGA were selected for verification [see Additional file 8]. Compared with normal liver tissues, hsa-miR-216b-5p (SMD = 0.593, $P = 0.000$, Fig. 6a), hsa-miR-107 (SMD = 0.729, $P = 0.000$, Fig. 6b), hsa-miR-17-5p (SMD = 0.502, $P = 0.001$, Fig. 6c) were up-regulated in HCC tissues, while has-miR-125a-5p (SMD = -0.947, $P = 0.000$, Fig. 6d), hsa-miR-22-3p (SMD = -0.563, $P = 0.000$, Fig. 6e) were down-regulated in HCC tissues. In addition, hsa-miR-20b-5p (SMD = 0.194, $P = 0.217$, Fig. 6f) and hsa-miR-142-3p (SMD = -0.425, $P = 0.056$, Fig. 6g) were not differentially expressed between normal tissues and HCC tissues, more studies with larger sample size were still needed.

We analyzed the correlation between the expression of FBXL19-AS1 and these 7 miRNAs based on the TCGA LIHC dataset. Significant correlations were not found in hsa-miR-216b-5p (r = -0.0010, $P = 0.9830$, Fig. 7a), hsa-miR-107 (r = -0.0504, $P = 0.3027$, Fig. 7b), hsa-miR-17-5p (r = 0.0715, $P = 0.1438$, Fig. 7c) or hsa-miR-125a-5p (r = 0.0303, $P = 0.5357$, Fig. 7d), but the relations were prominent in hsa-miR-22-3p (r = -0.2861, $P < 0.001$, Fig. 7e), hsa-miR-20b-5p (r = 0.0993, $P = 0.0420$, Fig. 7f) and hsa-miR-142-3p (r = -0.1435, $P = 0.0032$, Fig. 7g). Hence, we took hsa-miR-22-3p, hsa-miR-20b-5p and hsa-miR-142-3p for subsequent analyses.

LncRNA-miRNA-mRNA network construction

To further explore the potential downstream targets of these 3 miRNAs, three online bioinformatics servers (miRDB, miRTarBase and TargetScan) were used. There were 399 target genes of these 3 miRNAs simultaneously supported by all three databases. Then, we screened out 12,841 differentially expressed mRNAs in TCGA LIHC ($P < 0.05$). In addition, 12,194 mRNAs were predicted to be co-expressed with FBXL19-AS1 in HCC by cBioportal database ($P < 0.05$). Finally, 205 mRNAs were selected as targets through the intersection of the above three gene sets.

A new ceRNA network was formed among lncRNA (FBXL19-AS1), three miRNAs (hsa-miR-22-3p, hsa-miR-20b-5p, hsa-miR-142-3p) and 205 mRNAs (Fig. 8a). The diamond in the middle represented FBXL19-AS1, the gray triangles were miRNAs, and the circles were mRNAs. The circles in red meant the corresponding mRNAs were elevated in HCC, blue circles represented the decreased expression of related mRNA in HCC, deeper color indicated increased logFC, and larger size indicated smaller *P* value.

PPI network construction and screening of hub genes

We constructed a PPI network of these 205 mRNAs based on the STRING database and then visualized by Cytoscape 3.7.2. After removing the free nodes, the PPI network containing 158 nodes and 272 edges (Fig. 8b). Thereafter, hub genes identified by 12 algorithms (MCC、DMNC、MNC、Degree、EPC、BottleNeck、EcCentricity、Closeness、Radiality、Betweenness、Stress、ClusteringCoefficient) constituted a subnetwork with 9 nodes and 9 edges (Fig. 8c), which revealed the 9 hub genes (STAT3, CNOT7 BTG3, E2F1, TRIM37, YWHAZ, RBBP7, KIF23, ESR1) played important roles in the pathogenesis of HCC.

Functional analysis of 9 hub genes

GO and KEGG enrichment analyses were performed on the 9 hub genes ($P < 0.05$). Top 15 terms and pathways were selected for demonstration by *P* value. GO functional enrichment analysis revealed hub genes mainly enriched in transcription factor activity and transcriptional activator activity (Fig. 9a, Table 4). KEGG pathway analysis indicated the 9 hub genes might influence the occurrence and progression of HCC by participating in pathways such as hepatitis C, hepatitis B, microRNAs in cancer, cell cycle, viral carcinogenesis, and proteoglycans in cancer (Fig. 9b, Table 5). In addition, the 9 hub genes were also involved in pathways associated with non-small cell lung cancer, pancreatic cancer, breast cancer and other diseases.

Verification of ceRNA network

In order to establish a more reliable ceRNA network, we performed correlation analyses among FBXL19-AS1, 2 miRNAs and 9 mRNAs based on 370 HCC tissues and 50 normal tissues from TCGA LIHC dataset. Considering none of the 9 hub genes was correlated with hsa-miR-142-3p, it was not enrolled into the subsequent analyses. Significant correlations were found in FBXL19-AS1, hsa-miR-22-3p, hsa-miR-20b-5p, and 7 mRNAs, except STAT3 and CNOT9 (Fig. 10). Survival analyses of OS and DFS of the remaining 7 hub genes were performed by the Kaplan-Meier method in the GEPIA2 database. Remarkable survival differences existed in nearly all the 7 hub genes, except the DFS of YWHAZ (Fig. 11), which indicated all

the 7 hub genes were associated with the prognosis of HCC. Therefore, we constructed a ceRNA network consisting of 1 lncRNA, 2 miRNAs, 7 hub genes, and seven lncRNA-miRNA-mRNA regulatory pathways (FBXL19-AS1/miR-22-3p/YWHAZ axis, FBXL19-AS1/miR-22-3p/ESR1 axis, FBXL19-AS1/miR-20b-5p/E2F1 axis, FBXL19-AS1/miR-20b-5p/BTG3 axis, FBXL19-AS1/miR-20b-5p/KIF23 axis, FBXL19-AS1/miR-20b-5p/KIF23 axis, FBXL19-AS1/miR-20b-5p/TRIM37 axis, FBXL19-AS1/miR-20b-5p/RBBP7 axis) (Fig. 12A). To further verify the reliability of the network, we analyzed the expression status of the elements in the network based on TCGA LIHC dataset. As shown in Fig. 12B, FBXL19-AS1, has-miR-20b-5p, has-miR-22-3p and 7 hub genes were all differentially expressed between normal tissues and HCC tissues.

Discussion

In our study, FBXL19-AS1 was identified as a potential oncogene through integrated analysis of 6 GEO microarray datasets and TCGA LIHC dataset. Previous studies have shown that FBXL19-AS1 is significantly increased in breast cancer [9–10, 28], lung cancer [11–12, 29], osteosarcoma [13] and colorectal cancer [14], and participates in the migration, proliferation and survival of tumor cells. The underlying function of FBXL19-AS1 in HCC has not been studied yet. To verify the bioinformatics results and explore the role of FBXL19-AS1 played in HCC, qPCR was used to assess that the expression status of FBXL19-AS1. The experimental results indicated FBXL19-AS1 was elevated in HCC and its expression was correlated with TNM stage, AFP and GGT. Given that elevated GGT is associated with the occurrence of acute and chronic hepatitis and alcoholic liver disease, it can be inferred that FBXL19-AS1 may be involved in the development of related diseases. In combination with the GEPIA2 survival analysis results and our follow-up study on 57 patients, we found high expression of FBXL19-AS1 was associated with poor prognosis in HCC.

Biomarkers screened from liver tissues are not suitable for early diagnosis of HCC, and the specificity and sensitivity of AFP, the most widely used plasma biomarker in HCC diagnosis, are quite limited. In order to make up for the deficiency of early diagnosis of HCC, we evaluated the diagnostic value of plasma FBXL19-AS1. The results showed that the plasma FBXL19-AS1 in patients with hepatitis B, cirrhosis and HCC was significantly higher than that of healthy subjects. ROC analysis revealed plasma FBXL19-AS1 was with satisfactory diagnostic value in differentiating healthy controls from patients with hepatitis B, cirrhosis and especially HCC. Whereas, the discernibility ability of FBXL19-AS1 in hepatitis B patients and cirrhosis patients was unsatisfactory, which could be partially explained by the pathological similarity of the patients. It should be noted that the combination of plasma FBXL19-AS1 and AFP could significantly improve the diagnosis for HCC, suggesting that FBXL19-AS1 could serve as a biomarker for the auxiliary diagnosis of HCC. it is also important to note that FBXL19-AS1 has been reported to be associated with a variety of cancers, and therefore the need to combine FBXL19-AS1 and AFP to enhance the diagnostic specificity of HCC should be emphasized.

FBXL19-AS1 mainly locates in cytosol, suggesting FBXL19-AS1 may function as miRNA sponge to regulate mRNA expression indirectly. The potential interactions between FBXL19-AS1 and 7 miRNAs (has-

miR-142-3p, hsa-miR-125a-5p, hsa-miR-216b-5p, hsa-miR-107, hsa-miR-17-5p, has-miR-20b-5p, has-miR-22-3p) were revealed through multi-step bioinformatics analyses. Encouragingly, compared with normal liver tissues, the expressions of hsa-miR-216b-5p, hsa-miR-107 and hsa-miR-17-5p were up-regulated in HCC, and the expressions of hsa-miR-125a-5p and hsa-miR-22-3p were down-regulated in HCC. The expressions of hsa-miR-125a-5p, hsa-miR-107, hsa-miR-17-5p and hsa-miR-22-3p in HCC were consistent with published studies [30–33]. However, several studies have come up with results that were ambivalent with ours in hsa-miR-216b-5p, hsa-miR-142-3p and hsa-miR-20b-5p [34–36]. Since the heterogeneity of cross-studies cannot be ignored and the credibility of the combined results may decrease due to interfusion of the low-quality studies, more studies are needed to verify these results.

We analyzed the correlation between FBXL19-AS1 and these 7 miRNAs based on TCGA LIHC dataset, and finally selected 3 miRNAs (hsa-miR-22-3p, hsa-miR-20b-5p, hsa-miR-142-3p) that met our standards for subsequent analysis. Further studies revealed that FBXL19-AS1 may act as ceRNA to competitively bind to the above 3 miRNAs and regulate the expression of 205 mRNAs. In order to elucidate the ceRNA regulatory mechanism, we established a PPI network and obtained 9 hub genes (STAT3, CNOT7 BTG3, E2F1, TRIM37, YWHAZ, RBBP7, KIF23, ESR1). GO functional annotation and KEGG pathway analysis revealed the 9 hub genes were enriched in hepatitis B associated pathways and the important roles of these 9 hub genes in HCC have also been confirmed [37–45]. However, the relationship between the 9 hub genes and FBXL19-AS1 has not been reported. Through correlation analysis based on 420 TCGA LIHC tissue samples, STAT3 and CNOT7 were excluded, and the remaining 7 mRNAs were all associated with the prognosis of HCC. Finally, we constructed a more reliable ceRNA network consisting of FBXL19-AS1, hsa-miR-22-3p, hsa-miR-20b-5p, 7 hub genes (BTG3, E2F1, TRIM37, YWHAZ, RBBP7, KIF23, ESR1), and 7 lncRNA-miRNA-mRNA regulatory axes. A study reported miR-22 and miR-20b were involved in the progression of HBV-related HCC which further improved the credibility of our research [46]. Intriguingly, we found FBXL19, the complementary gene of FBXL19-AS1, was associated with tumor immune invasion according to TIMER database. Thus, we speculated FBXL19-AS1 might form RNA-RNA dimer with FBXL19 through the classical pattern, which might affect the expression of FBXL19 and affected the immune infiltration in HCC.

Conclusions

In summary, FBXL19-AS1 was identified as an oncogenic lncRNA that may serve as a diagnostic and prognostic agent for HCC potential biomarkers. We also established a FBXL19-AS1-miRNA-mRNA network, and demonstrated that FBXL19-AS1 might participate in the pathological progression of HCC as a ceRNA. Our study elucidates the potential oncogenic pathways involved in FBXL19-AS1 and recognizes the role of FBXL19-AS1 in the possible target genes in HCC. Our findings might provide new perspectives on the pathogenesis of HCC, thus broadening the therapeutic options for HCC.

List Of Abbreviations

HCC: hepatocellular carcinoma; FBXL19-AS1: F-box and leucine-rich repeat protein 19-antisense RNA 1; ceRNA: competing endogenous RNA; AFP: alpha-fetoprotein; ncRNAs: non-coding RNAs; MiRNAs: microRNAs; LncRNAs: long non-coding RNAs; MREs: miRNA response elements; TCGA LIHC: The Cancer Genome Atlas liver hepatocellular carcinoma; GEO: Gene Expression Omnibus; GSEA: Gene Set Enrichment Analysis; AJCC: American Joint Committee on Cancer; CDNA: complementary DNA; qPCR: quantitative real-time PCR; GAPDH: glyceraldehyde 3-phosphate dehydrogenase; ALT: alanine aminotransferase; AST: aspartate aminotransferase; GGT: γ-Glutamyl Transferase; CEA: carcinoembryonic antigen; HBV: hepatitis B virus; TP: total protein; ALB: albumin; ALP: alkaline phosphatase; GLU: glucose; AUC: area under the curve; Se: sensitivity; Sp: specificity. GEPIA2: Gene Expression Profiling Interactive Analysis2; SMD: standard mean difference; 95% CI: 95% confidence interval; GO: Gene Ontology; KEGG: Kyoto Encyclopedia of Genes and Genomes; SD: standard deviation; ROC: Receiver operation curve; TIICs: tumor infiltrating immune cells.

Declarations

Ethics approval and consent to participate

All experimental schemes were approved by the Ethics Committee of Zhongnan Hospital of Wuhan University.

Consent for publication

Not applicable.

Availability of data and materials

The datasets used and/or analyzed during the current study are available from the corresponding author on reasonable request.

Competing interests

The authors declare that they have no competing interests.

Funding

This work was supported by grants of the National Basic Research Program of China (2012CB720605) and Zhongnan Hospital of Wuhan University Science, Technology and Innovation Seed Fund (ZNPY2017054).

Authors' contributions

DDH and JCT designed the workflow and wrote this paper. XKZ, XYZ, NM performed the experiments, analyzed the data. YCW and PL collected the samples. CZL revised the manuscript. All authors approved the final manuscript.

Acknowledgements

Not applicable.

References

1. Bray F, Ferlay J, Soerjomataram I, Siegel RL, Torre LA, Jemal A. Global cancer statistics 2018: GLOBOCAN estimates of incidence and mortality worldwide for 36 cancers in 185 countries. Cancer J Clin. 2018;68:394–424.
2. Greten TF, Lai CW, Li G, Staveley-O'Carroll KF. Targeted and Immune-Based Therapies for Hepatocellular Carcinoma. Gastroenterology. 2019;156:510–24.
3. Kulik L, El-Serag HB. Epidemiology and Management of Hepatocellular Carcinoma. Gastroenterology. 2019;156:477 – 91.e471..
4. Takagi K, Yagi T, Umeda Y, et al. Preoperative Controlling Nutritional Status (CONUT) Score for Assessment of Prognosis Following Hepatectomy for Hepatocellular Carcinoma. World journal of surgery. 2017;41:2353–60.
5. Allemani C, Matsuda T, Di Carlo V, et al. Global surveillance of trends in cancer survival 2000-14 (CONCORD-3): analysis of individual records for 37†513†025 patients diagnosed with one of 18 cancers from 322 population-based registries in 71 countries. 391. London: Lancet; 2018. pp. 1023–75.
6. Forner A, Reig M, Bruix J. Hepatocellular carcinoma. Lancet. 2018;391:1301–14.
7. Klingenberg M, Matsuda A, Diederichs S, Patel T. Non-coding RNA in hepatocellular carcinoma: Mechanisms, biomarkers and therapeutic targets. Journal of hepatology. 2017;67:603–18.
8. Salmena L, Poliseno L, Tay Y, Kats L, Pandolfi PP. A ceRNA hypothesis: the Rosetta Stone of a hidden RNA. language? Cell. 2011;146:353–8.
9. Dong G, Pan T, Zhou D, Li C, Liu J, Zhang J. FBXL19-AS1 promotes cell proliferation and inhibits cell apoptosis via miR-876-5p/FOXM1 axis in breast cancer. Acta Biochim Biophys Sin. 2019;51:1106–13.
10. Ding Z, Ye P, Yang X, Cai H. LncRNA FBXL19-AS1 promotes breast cancer cells proliferation and invasion via acting as a molecular sponge to miR-718. Bioscience reports. 2019;39.
11. Jiang Q, Cheng L, Ma D, Zhao Y. FBXL19-AS1 exerts oncogenic function by sponging miR-431-5p to regulate RAF1 expression in lung cancer. Bioscience reports. 2019;39.
12. Wang L, Zhang X, Liu Y, Xu S. Long noncoding RNA FBXL19-AS1 induces tumor growth and metastasis by sponging miR-203a-3p in lung adenocarcinoma. Journal of cellular physiology. 2020;235:3612–25.
13. Pan R, He Z, Ruan W, et al. lncRNA FBXL19-AS1 regulates osteosarcoma cell proliferation, migration and invasion by sponging miR-346. OncoTargets therapy. 2018;11:8409–20.

14. Shen B, Yuan Y, Zhang Y, et al. Long non-coding RNA FBXL19-AS1 plays oncogenic role in colorectal cancer by sponging miR-203. Biochem Biophys Res Commun. 2017;488:67–73.
15. Blum A, Wang P, Zenklusen JC. SnapShot: TCGA-Analyzed Tumors. Cell. 2018;173:530.
16. Barrett T, Wilhite SE, Ledoux P, et al. NCBI GEO: archive for functional genomics data sets–update. Nucleic acids research. 2013;41:D991-5.
17. Cao Z, Pan X, Yang Y, Huang Y, Shen HB. The lncLocator: a subcellular localization predictor for long non-coding RNAs based on a stacked ensemble classifier. Bioinformatics. 2018;34:2185–94.
18. Leek JT, Johnson WE, Parker HS, Jaffe AE, Storey JD. The sva package for removing batch effects and other unwanted variation in high-throughput experiments. Bioinformatics. 2012;28:882–3.
19. Ritchie ME, Phipson B, Wu D, et al. limma powers differential expression analyses for RNA-sequencing and microarray studies. Nucleic acids research. 2015;43:e47.
20. Robinson MD, McCarthy DJ, Smyth GK. edgeR: a Bioconductor package for differential expression analysis of digital gene expression data. Bioinformatics. 2010;26:139–40.
21. Subramanian A, Tamayo P, Mootha VK, Mukherjee S, Ebert BL, Gillette MA, et al. Gene set enrichment analysis: a knowledge-based approach for interpreting genome-wide expression profiles. Proc Natl Acad Sci USA. 2005;102:15545–50.
22. Tang Z, Kang B, Li C, Chen T, Zhang Z. GEPIA2: an enhanced web server for large-scale expression profiling and interactive analysis. Nucleic acids research. 2019;47:W556-60.
23. Franceschini A, Szklarczyk D, Frankild S, et al. STRING v9.1: protein-protein interaction networks, with increased coverage and integration. Nucleic acids research. 2013;41:D808-15.
24. Chin CH, Chen SH, Wu HH, Ho CW, Ko MT, Lin CY. cytoHubba: identifying hub objects and sub-networks from complex interactome. BMC systems biology. 2014;8(Suppl 4):11.
25. Yu G, Wang LG, Han Y, He QY. clusterProfiler: an R package for comparing biological themes among gene clusters. Omics: a journal of integrative biology. 2012;16:284–7.
26. Gene Ontology Consortium. going forward. Nucleic acids research. 2015;43:D1049-56.
27. Kanehisa M, Furumichi M, Tanabe M, Sato Y, Morishima K. KEGG: new perspectives on genomes, pathways, diseases and drugs. Nucleic acids research. 2017;45:D353-61.
28. Zhang Y, Xiao X, Zhou W, Hu J, Zhou D. LIN28A-stabilized FBXL19-AS1 promotes breast cancer migration, invasion and EMT by regulating WDR66. vitro cellular developmental biology Animal. 2019;55:426–35.
29. Yu DJ, Li YH, Zhong M. LncRNA FBXL19-AS1 promotes proliferation and metastasis via regulating epithelial-mesenchymal transition in non-small cell lung cancer. Eur Rev Med Pharmacol Sci. 2019;23:4800–6.
30. Xu X, Tao Y, Niu Y, et al. miR-125a-5p inhibits tumorigenesis in hepatocellular carcinoma. Aging. 2019;11:7639–62.
31. Su SG, Yang M, Zhang MF, et al. miR-107-mediated decrease of HMGCS2 indicates poor outcomes and promotes cell migration in hepatocellular carcinoma. Int J Biochem Cell Biol. 2017;91:53–9.

32. Yang F, Yin Y, Wang F, et al. miR-17-5p Promotes migration of human hepatocellular carcinoma cells through the p38 mitogen-activated protein kinase-heat shock protein 27 pathway. Hepatology. 2010;51:1614–23.
33. Zhao L, Hu K, Cao J, et al. lncRNA miat functions as a ceRNA to upregulate sirt1 by sponging miR-22-3p in HCC cellular senescence. Aging. 2019;11:7098–122.
34. Dai Q, Deng J, Zhou J, et al. Long non-coding RNA TUG1 promotes cell progression in hepatocellular carcinoma via regulating miR-216b-5p/DLX2 axis. Cancer cell international. 2020;20:8.
35. Zhang K, Chen J, Zhou H, et al. PU.1/microRNA-142-3p targets ATG5/ATG16L1 to inactivate autophagy and sensitize hepatocellular carcinoma cells to sorafenib. Cell death disease. 2018;9:312.
36. Xue TM, Tao LD, Zhang M, et al. Clinicopathological Significance of MicroRNA-20b Expression in Hepatocellular Carcinoma and Regulation of HIF-1α and VEGF Effect on Cell Biological Behaviour. Disease markers. 2015;2015:325176.
37. Grohmann M, Wiede F, Dodd GT, et al. Obesity Drives STAT-1-Dependent NASH and STAT-3-Dependent HCC. Cell. 2018;175:1289 – 306.e1220..
38. Ren C, Ren X, Cao D, et al. CNOT7 depletion reverses natural killer cell resistance by modulating the tumor immune microenvironment of hepatocellular carcinoma. FEBS open bio. 2020;10:847–60.
39. Wang L, Mo H, Jiang Y, et al. MicroRNA-519c-3p promotes tumor growth and metastasis of hepatocellular carcinoma by targeting BTG3. Biomedicine & pharmacotherapy = Biomedecine & pharmacotherapie. 2019;118:109267.
40. Chen Q, Wang L, Jiang M, et al. E2F1 interactive with BRCA1 pathway induces HCC two different small molecule metabolism or cell cycle regulation via mitochondrion or CD4 + T to cytosol. Journal of cellular physiology. 2018;233:1213–21.
41. Jiang J, Yu C, Chen M, Tian S, Sun C. Over-expression of TRIM37 promotes cell migration and metastasis in hepatocellular carcinoma by activating Wnt/β-catenin signaling. Biochem Biophys Res Commun. 2015;464:1120–7.
42. Zhao JF, Zhao Q, Hu H, et al. The ASH1-miR-375-YWHAZ Signaling Axis Regulates Tumor Properties in Hepatocellular Carcinoma. Molecular therapy Nucleic acids. 2018;11:538–53.
43. Chen H, Gao F, He M, et al. Long-Read RNA Sequencing Identifies Alternative Splice Variants in Hepatocellular Carcinoma and Tumor-Specific Isoforms. Hepatology (Baltimore, Md). 2019;70:1011–25.
44. Sun X, Jin Z, Song X, et al. Evaluation of KIF23 variant 1 expression and relevance as a novel prognostic factor in patients with hepatocellular carcinoma. BMC Cancer. 2015;15:961.
45. Dou CY, Fan YC, Cao CJ, Yang Y, Wang K. Sera DNA Methylation of CDH1, DNMT3b and ESR1 Promoters as Biomarker for the Early Diagnosis of Hepatitis B Virus-Related Hepatocellular Carcinoma. Digestive diseases sciences. 2016;61:1130–8.
46. Wang G, Dong F, Xu Z, et al. MicroRNA profile in HBV-induced infection and hepatocellular carcinoma. BMC Cancer. 2017;17:805.

Tables

Table 1 Relationship between FBXL19-AS1 expression in tissues and clinical characteristics of HCC patients.

Characteristics	Patient number (n = 57)	Fold change (%)		*P* value
		Low (n = 28)	High (n = 29)	
Gender:				1.000
Female	4	2	2	
Male	53	26	27	
Age (y):				0.889
< 55	30	15	15	
≥ 55	27	13	14	
Smoking:				0.705
Positive	34	16	18	
Negative	23	12	11	
Alcoholism:				0.503
Positive	27	12	15	
Negative	30	16	14	
Tumor size (cm)				0.227
< 5	20	12	8	
≥ 5	37	16	21	
Tumor nodes:				1.000
Single	52	26	26	
Multi	5	2	3	
TNM:				**0.043**
I/II	21	14	7	
III/IV	36	14	22	
Histologic grade:				0.275
Well and moderate	49	26	23	
Low	8	2	6	
ALT (U/l):				0.223
< 46	32	18	14	
≥ 46	25	10	15	
AST (U/l):				0.083
< 46	30	18	12	
≥ 46	27	10	17	
GGT (U/l):				**0.046**
< 55	23	15	8	
≥ 55	34	13	21	
AFP (ng/l):				**0.020**
< 200	34	21	13	
≥ 200	23	7	16	
CEA:				0.967
< 5	52	25	27	
≥ 5	5	3	2	
HBV DNA (IU/ml):				0.190
< 500	19	7	12	
≥ 500	38	21	17	

ALT, alanine aminotransferase; AST, aspartate aminotransferase; GGT, γ-Glutamyl Transferase; AFP, alpha-fetoprotein; CEA, carcinoembryonic antigen; HBV, hepatitis B virus.

Table 2 The main clinical features of research subjects.

teristics	HCC N=92	Cirrhosis N=80	Hepatitis B N=77	Control N=79	*P* value
:					0.317
	72	54	58	54	
	20	26	19	25	
:					0.178
	37	25	35	37	
	55	55	42	42	
/l)	49.00 (28.75-76.25)	26.00 (20.00-36.00)	88.00 (42.00-252.00)	18.00 (14.00-33.00)	**0.001**
/l)	57.50 (33.00-146.25)	48.50 (36.25-61.00)	51.00 (38.00-124.00)	22.00 (18.00-28.00)	**0.001**
	63.50 (59.55-70.40)	61.65 (55.55-68.20)	63.40 (56.00-68.70)	68.30 (59.25-73.10)	0.052
l)	35.40 (31.50-39.10)	32.60 (25.50-38.35)	35.00 (31.10-41.50)	44.80 (43.05-46.65)	**0.001**
/l)	31.00 (21.75-64.75)	35.50 (19.75-92.50)	35.00 (21.00-65.00)	28.00 (20.00-46.50)	0.227
/l)	119.00 (85.50-216.00)	151.00 (101.00-213.00)	137.00 (93.50-152.50)	88.00 (75.75-153.00)	0.351
mol/l)	4.94 (4.56-6.25)	5.16 (4.87-5.76)	4.89 (4.48-5.25)	5.10 (4.61-5.73)	0.700
g/ml)	17.46 (2.92-310.48)	4.76 (2.25-14.57)	6.00 (2.41-26.11)	3.10 (1.99-4.53)	**0.001**
g/ml)	2.05 (1.36-2.61)	2.09 (1.35-2.74)	1.96 (1.39-2.63)	1.79 (1.22-2.44)	0.394

TP, total protein; ALB, albumin; ALP, alkaline phosphatase; GLU, glucose.

Table 3 ROC analysis of FBXL19-AS1 and AFP for subgroups.

oup	Biomarker	AUC	95% CI	*P* value	Se (%)	Sp (%)
ols vs hepatitis B	FBXL19-AS1	0.761	0.688-0.835	<0.001	51.95	87.34
	AFP	0.716	0.634-0.798	<0.001	49.35	94.94
	Combination	0.831	0.767-0.895	<0.001	62.34	94.94
ols vs cirrhosis	FBXL19-AS1	0.776	0.705-0.846	<0.001	85.00	60.76
	AFP	0.668	0.582-0.753	<0.001	40.00	100.00
	Combination	0.836	0.775-0.896	<0.001	83.75	68.35
ols vs HCC	FBXL19-AS1	0.875	0.825-0.924	<0.001	76.09	82.28
	AFP	0.769	0.699-0.839	<0.001	54.35	100.00
	Combination	0.931	0.895-0.967	<0.001	80.43	96.20
itis B vs cirrhosis	FBXL19-AS1	0.482	0.389-0.574	0.694	86.25	29.87
	AFP	0.460	0.370-0.551	0.390	37.50	70.13
	Combination	0.524	0.432-0.616	0.598	63.75	50.65
itis B vs HCC	FBXL19-AS1	0.635	0.551-0.719	0.003	94.57	29.87
	AFP	0.624	0.540-0.708	0.006	38.04	92.21
	Combination	0.702	0.624-0.779	<0.001	43.48	88.31
sis vs HCC	FBXL19-AS1	0.672	0.592-0.752	0.001	72.83	60.00
	AFP	0.654	0.572-0.735	<0.001	45.65	90.00
	Combination	0.673	0.593-0.753	<0.001	72.83	60.00

AUC, area under the curve; Se, sensitivity; Sp, specificity.

Table 4 List of top 15 enriched GO terms.

ID	Description	*P* value	Gene ID	Gene count
GO:0004879	nuclear receptor activity	2.80E-04	STAT3/ESR1	2
GO:0098531	transcription factor activity, direct ligand regulated sequence-specific DNA binding	2.80E-04	STAT3/ESR1	2
GO:0001077	transcriptional activator activity, RNA polymerase II proximal promoter sequence-specific DNA binding	3.72E-04	E2F1/STAT3/ESR1	3
GO:0035258	steroid hormone receptor binding	9.06E-04	STAT3/ESR1	2
GO:0000982	transcription factor activity, RNA polymerase II proximal promoter sequence-specific DNA binding	1.21E-03	E2F1/STAT3/ESR1	3
GO:0001228	transcriptional activator activity, RNA polymerase II transcription regulatory region sequence-specific DNA binding	1.23E-03	E2F1/STAT3/ESR1	3
GO:0001085	RNA polymerase II transcription factor binding	2.17E-03	STAT3/ESR1	2
GO:0035257	nuclear hormone receptor binding	2.55E-03	STAT3/ESR1	2
GO:0051427	hormone receptor binding	3.76E-03	STAT3/ESR1	2
GO:0030235	nitric-oxide synthase regulator activity	5.60E-03	ESR1	1
GO:0004535	poly(A)-specific ribonuclease activity	6.62E-03	CNOT7	1
GO:0035259	glucocorticoid receptor binding	7.13E-03	STAT3	1
GO:0005126	cytokine receptor binding	8.46E-03	STAT3/TRIM37	2
GO:0031625	ubiquitin protein ligase binding	8.75E-03	YWHAZ/TRIM37	2
GO:0044389	ubiquitin-like protein ligase binding	9.66E-03	YWHAZ/TRIM37	2

Table 5 List of top 15 enriched KEGG terms.

ID	Description	*P* value	Gene ID	Gene count
hsa05160	Hepatitis C	3.66E-04	E2F1/YWHAZ/STAT3	3
hsa05161	Hepatitis B	4.17E-04	E2F1/YWHAZ/STAT3	3
hsa05223	Non-small cell lung cancer	1.91E-03	E2F1/STAT3	2
hsa04917	Prolactin signaling pathway	2.02E-03	STAT3/ESR1	2
hsa05212	Pancreatic cancer	2.38E-03	E2F1/STAT3	2
hsa03018	RNA degradation	2.57E-03	BTG3/CNOT7	2
hsa05206	MicroRNAs in cancer	2.75E-03	E2F1/KIF23/STAT3	3
hsa01522	Endocrine resistance	3.92E-03	E2F1/ESR1	2
hsa04110	Cell cycle	6.22E-03	E2F1/YWHAZ	2
hsa05224	Breast cancer	8.65E-03	E2F1/ESR1	2
hsa05167	Kaposi sarcoma-associated herpesvirus infection	1.40E-02	E2F1/STAT3	2
hsa05169	Epstein-Barr virus infection	1.58E-02	E2F1/STAT3	2
hsa05203	Viral carcinogenesis	1.62E-02	YWHAZ/STAT3	2
hsa05205	Proteoglycans in cancer	1.64E-02	STAT3/ESR1	2
hsa05163	Human cytomegalovirus infection	1.95E-02	E2F1/STAT3	2

Additional Files

File name: Additional file 1

File format: .pdf

Title: Details of microarray datasets from GEO and TCGA.

Description: Additional file 1. Details of microarray datasets from GEO and TCGA.

File name: Additional file 2

File format: .pdf

Title: Primer sequence and Tm for qPCR.

Description: Additional file 2. Primer sequence and Tm for qPCR.

File name: Additional file 3

File format: .pdf

Title: Expression of 26 differentially expressed lncRNAs.

Description: Additional file 3. Expression of 26 differentially expressed lncRNAs.

File name: Additional file 4

File format: .pdf

Title: CeRNA network of 7 lncRNAs.

Description: Additional file 4. CeRNA network of 7 lncRNAs.

File name: Additional file 5

File format: .pdf

Title: Localization of FBXL19-AS in cells.

Description: Additional file 5. Localization of FBXL19-AS in cells.

File name: Additional file 6

File format: .pdf

Title: FBXL19 is associated with HCC immune infiltration.

Description: Additional file 6. FBXL19 is associated with HCC immune infiltration.

File name: Additional file 7

File format: .pdf

Title: Violin diagram of the relationship between FBXL19-AS1 and clinical stage.

Description: Additional file 7. Violin diagram of the relationship between FBXL19-AS1 and clinical stage.

File name: Additional file 8

File format: .pdf

Title: Essential information of the studies for the 7 miRNAs derived from GEO and TCGA database.

Description: Additional file 8. Essential information of the studies for the 7 miRNAs derived from GEO and TCGA database.

Figures

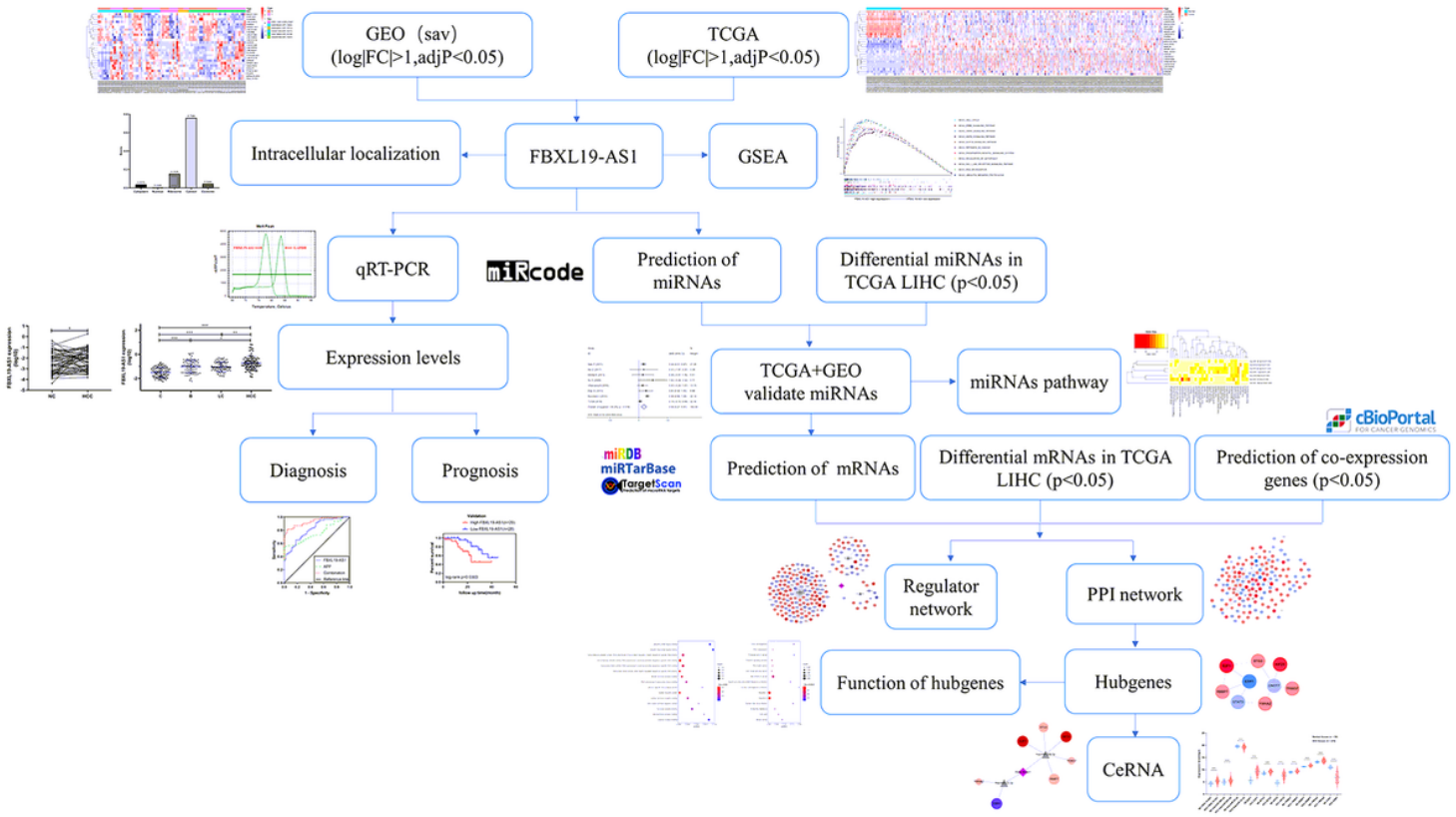

Figure 1

Flow diagram of the analysis process.

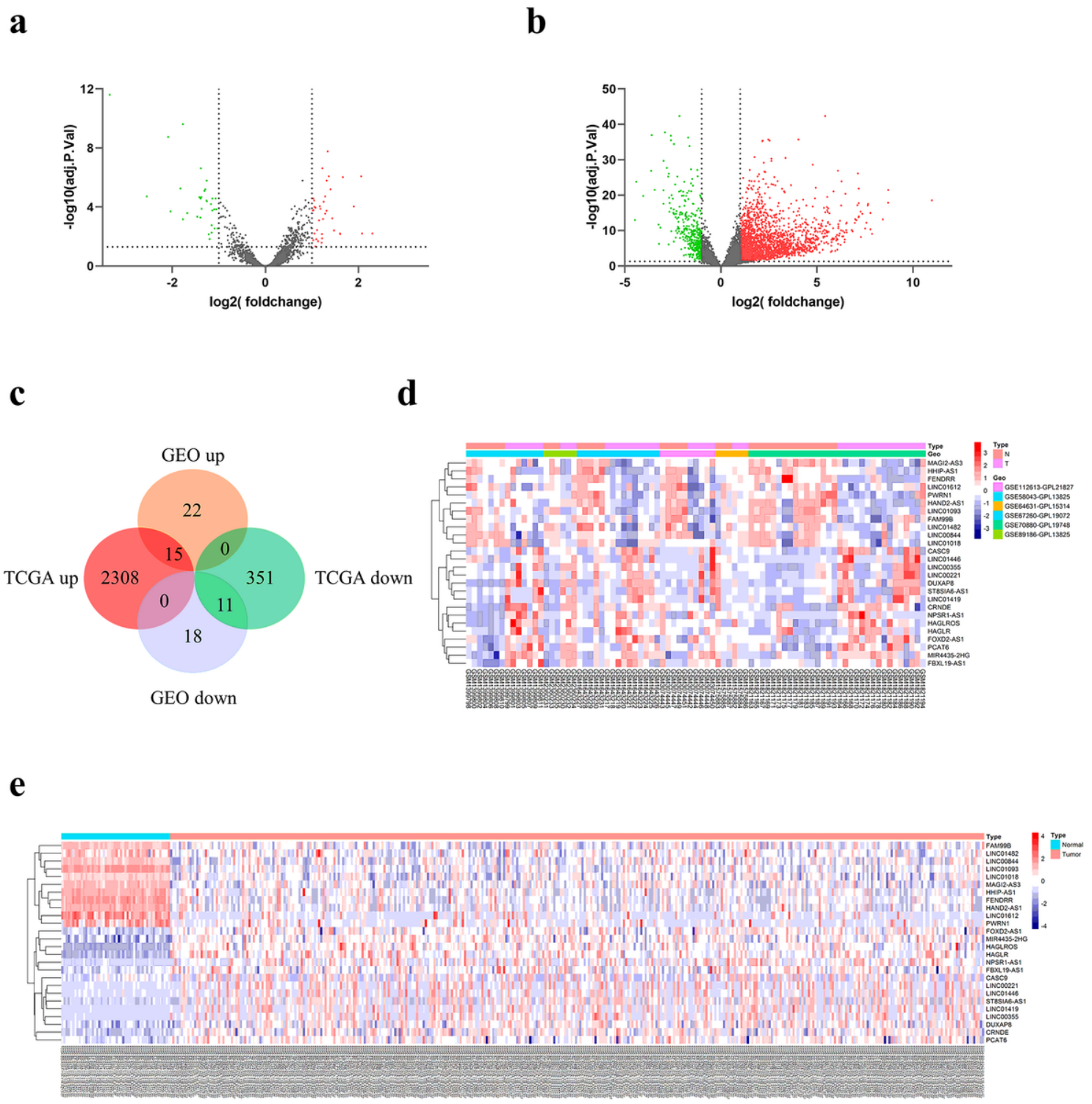

Figure 2

Identification of differentially expressed lncRNAs in HCC. a Volcano plots of differentially expressed lncRNAs identified from GEO joint dataset. b Volcano plots of differentially expressed lncRNAs identified from TCGA LIHC dataset. c Venn diagram for differentially expressed lncRNAs in GEO joint dataset and TCGA LIHC dataset. d Heatmap of 26 lncRNAs in GEO joint dataset. e Heatmap of 26 lncRNAs in TCGA LIHC dataset.

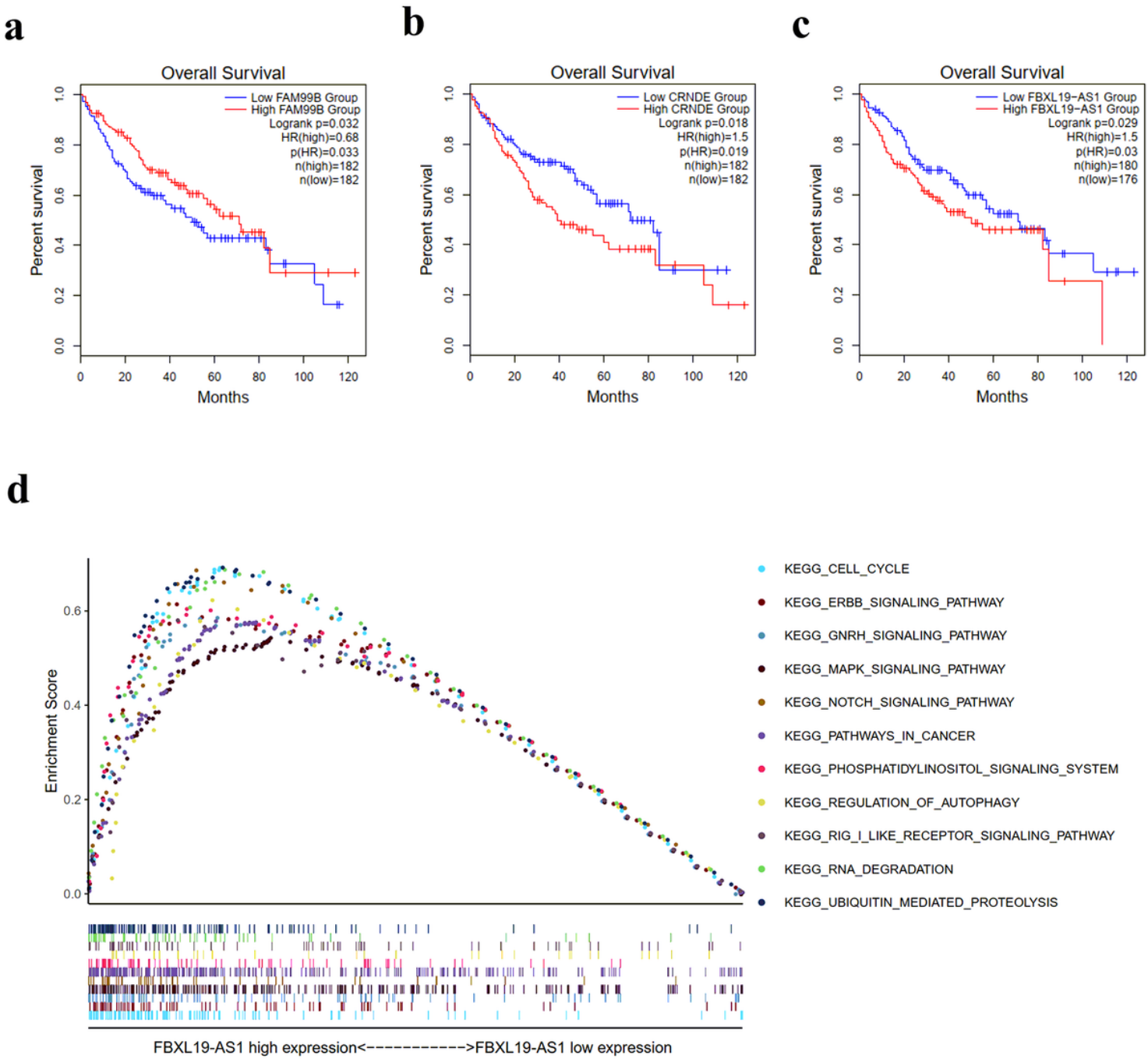

Figure 3

Kaplan-Meier survival analysis of lncRNAs based on TCGA LIHC and GSEA analysis on FBXL19-AS1. a Overall survival of FAM99B in HCC. b Overall survival of CRNDE in HCC. c Overall survival of FBXL19-AS1 in HCC. d GSEA analysis on FBXL19-AS1.

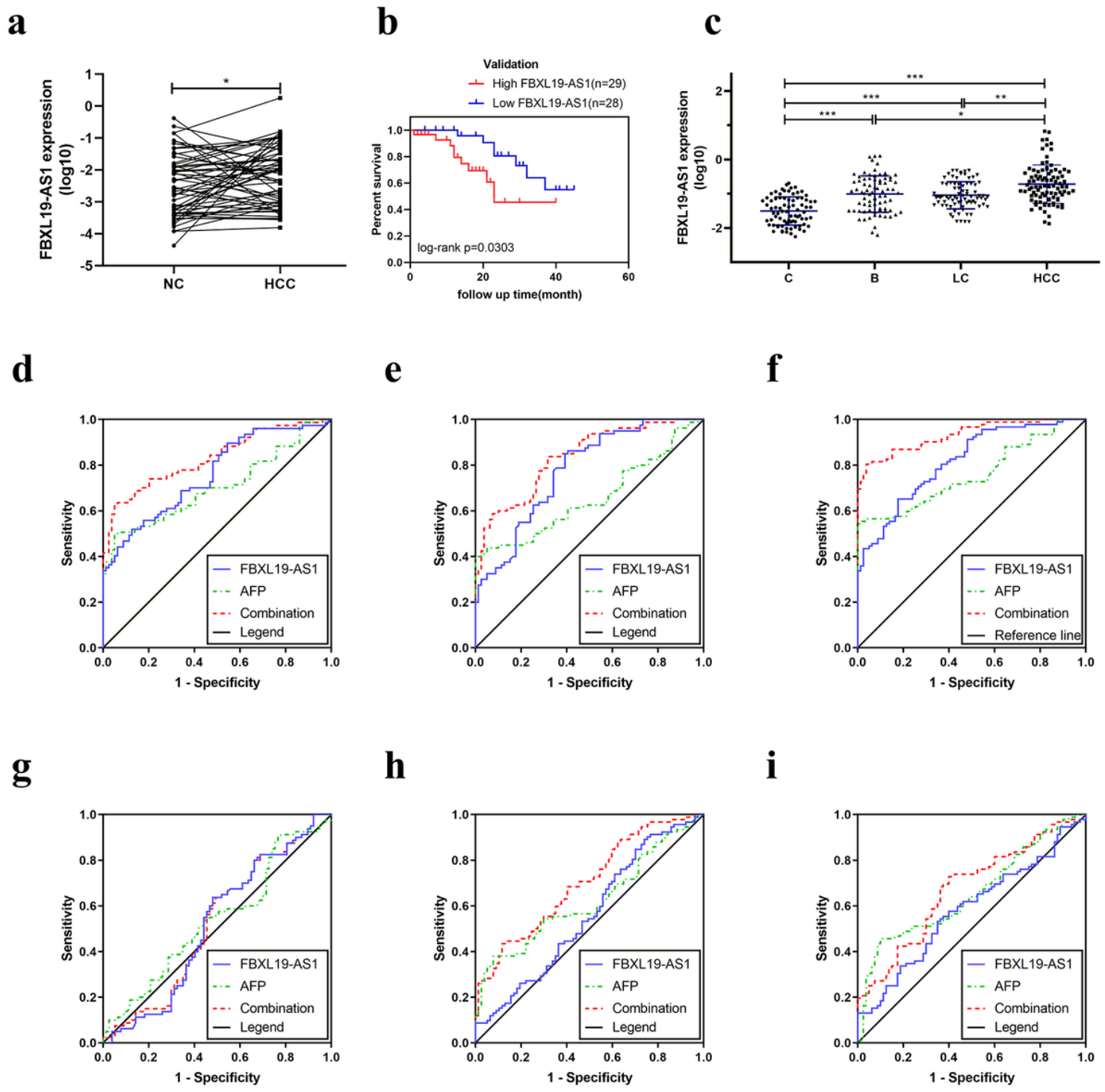

Figure 4

Expression of FBXL19-AS1 and its prognostic and diagnostic value. a The expression levels of FBXL19-AS1 in HCC tissues. b Overall survival of HCC patients with high (n = 29) or low (n = 28) FBXL19-AS1 levels in HCC tissues. c FBXL19-AS1 expression levels in plasma among the healthy control, hepatitis B, cirrhosis, and HCC groups. Data are presented as mean ± SD. d-i ROCs of FBXL19-AS1 and AFP in HCC. d Healthy control versus hepatitis B. e Healthy control versus cirrhosis. f Healthy control versus HCC. g

Hepatitis B versus cirrhosis. h Hepatitis B versus HCC. i Cirrhosis versus HCC. * P < 0.05, ** P < 0.01 and ***P<0.001.

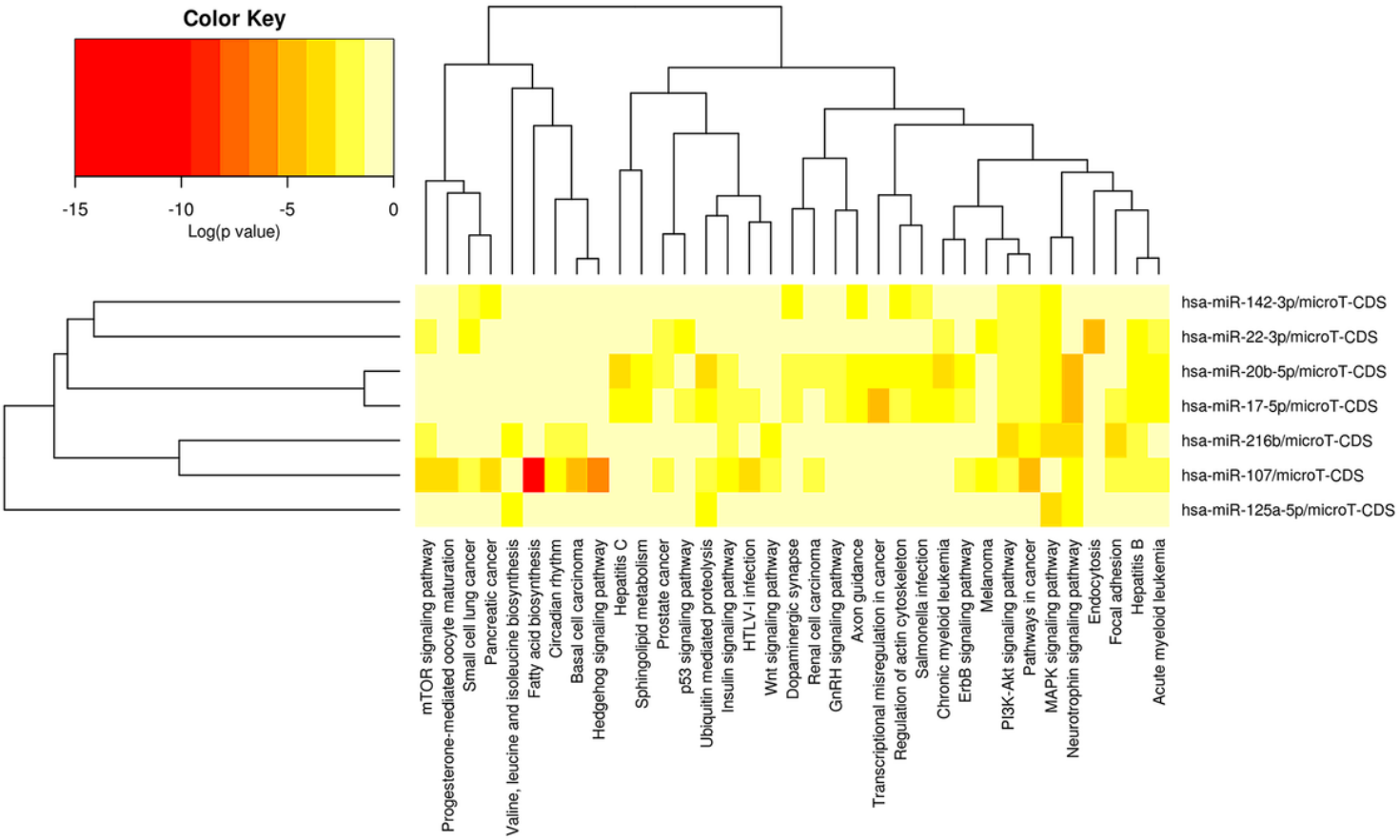

Figure 5

Heatmap for the signaling pathways from DIANA-miRPath in which the 7 miRNAs are involved.

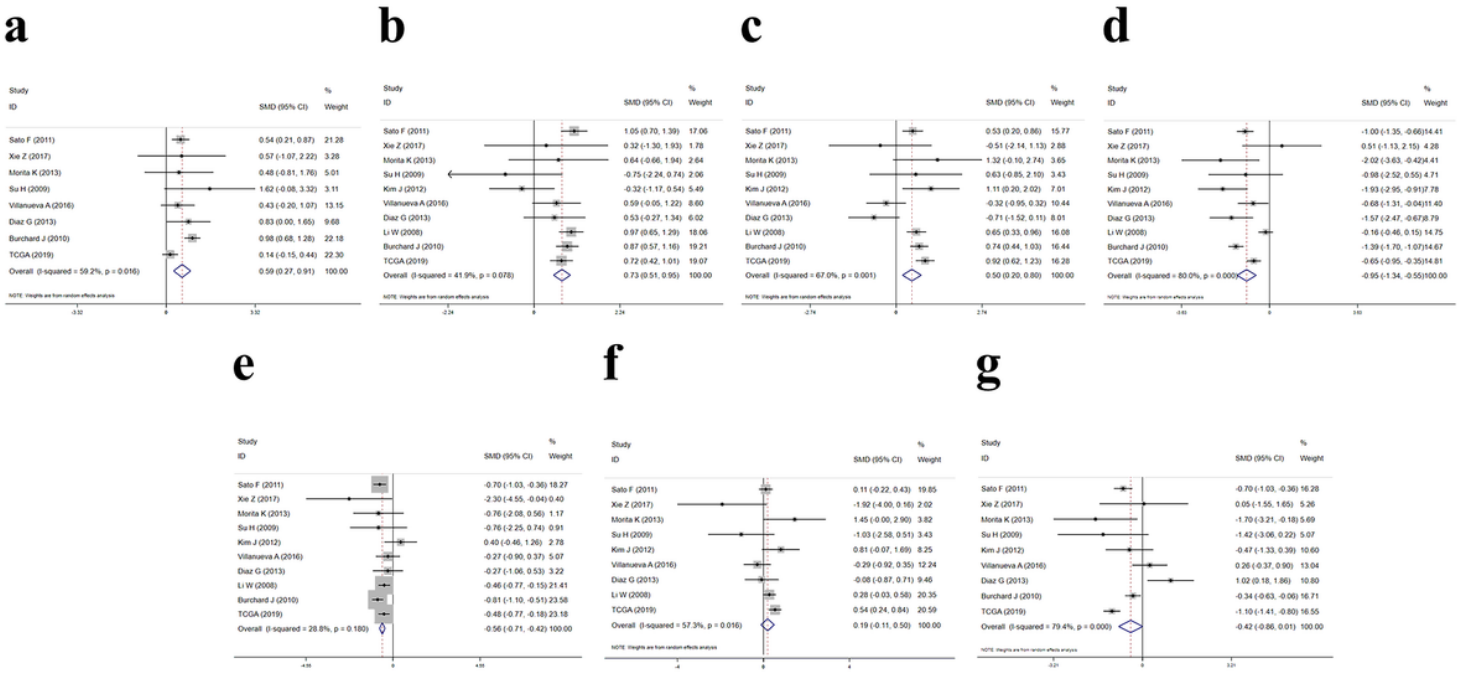

Figure 6

Forest diagrams of datasets assessing the levels of the predicted miRNAs in HCC. a has-miR-216b-5p. b has-miR-107. c has-miR-17-5p. d has-miR-125a-5p. e has-miR-22-3p. f has-miR-20b-5p. g has-miR-142-3p.

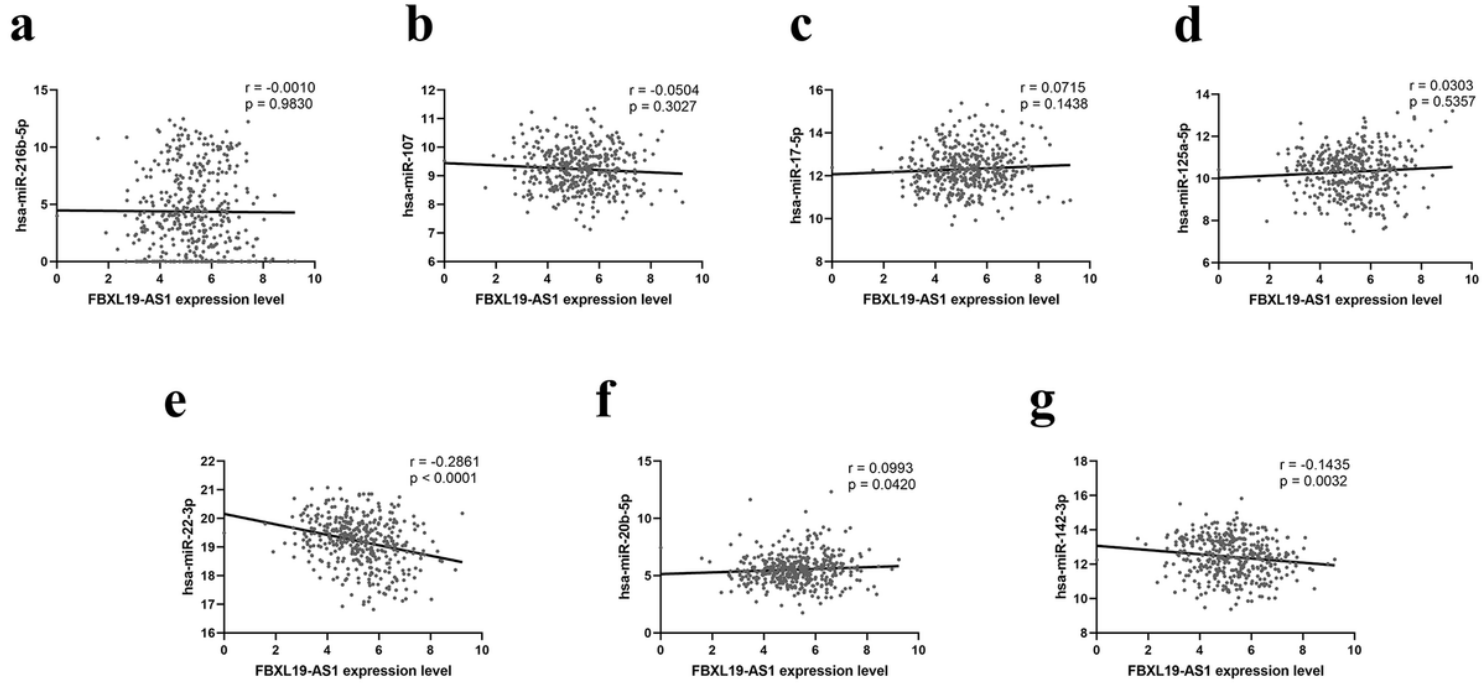

Figure 7

The correlation analysis between FBXL19-AS1 and 7 miRNAs. a has-miR-216b-5p. b has-miR-107. c has-miR-17-5p. d has-miR-125a-5p. e has-miR-22-3p. f has-miR-20b-5p. g has-miR-142-3p.

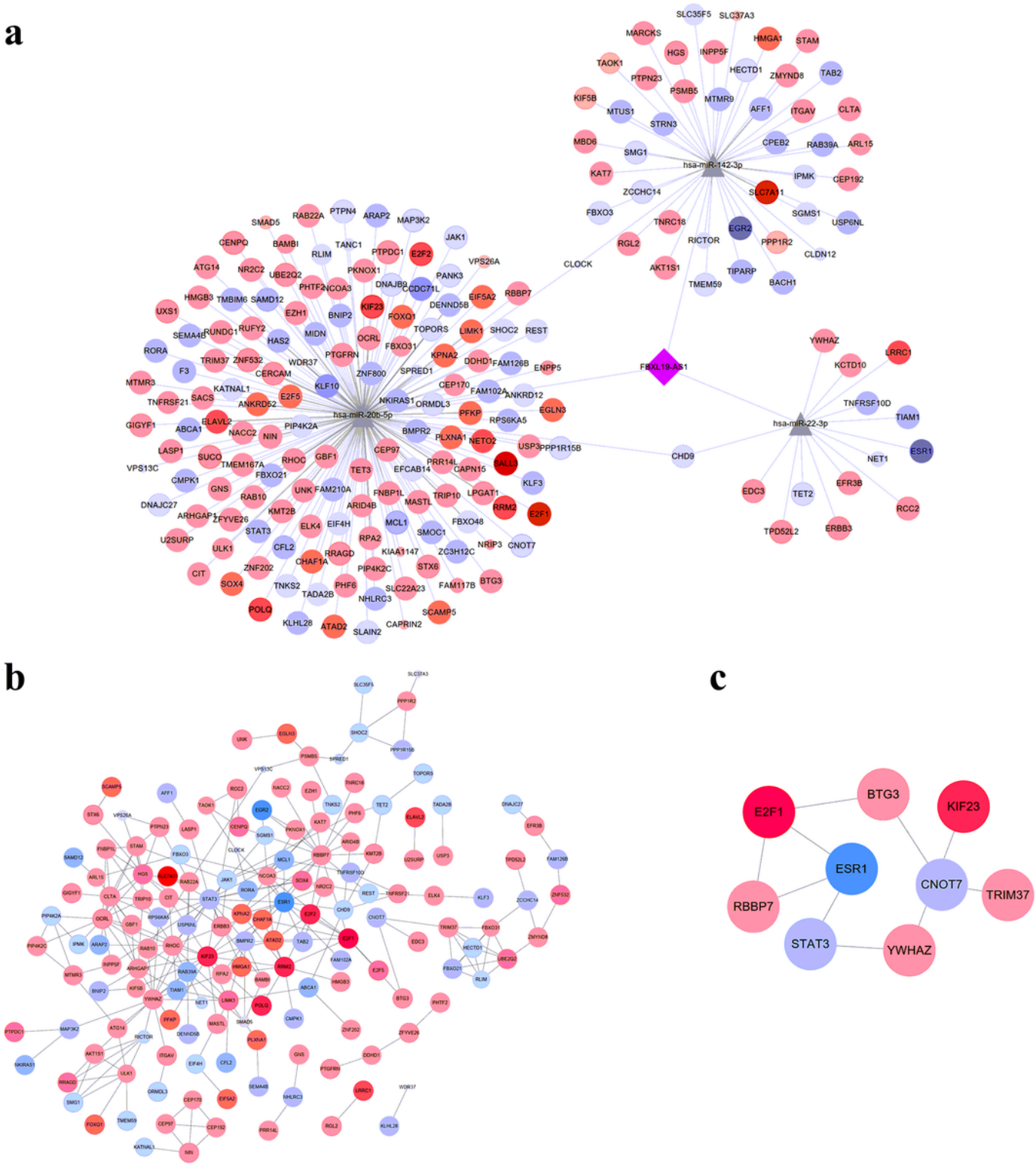

Figure 8

LncRNA-miRNA-mRNA network, PPI network and hub genes network. a The network including lncRNAs (FBXL19-AS1), 3 miRNAs (has-miR-22-3p, has-miR-20b-5p, has-miR-142-3p) and 205 mRNAs. b PPI network on these 205 mRNAs. c Hub genes network contained 9 nodes and 9 edges.

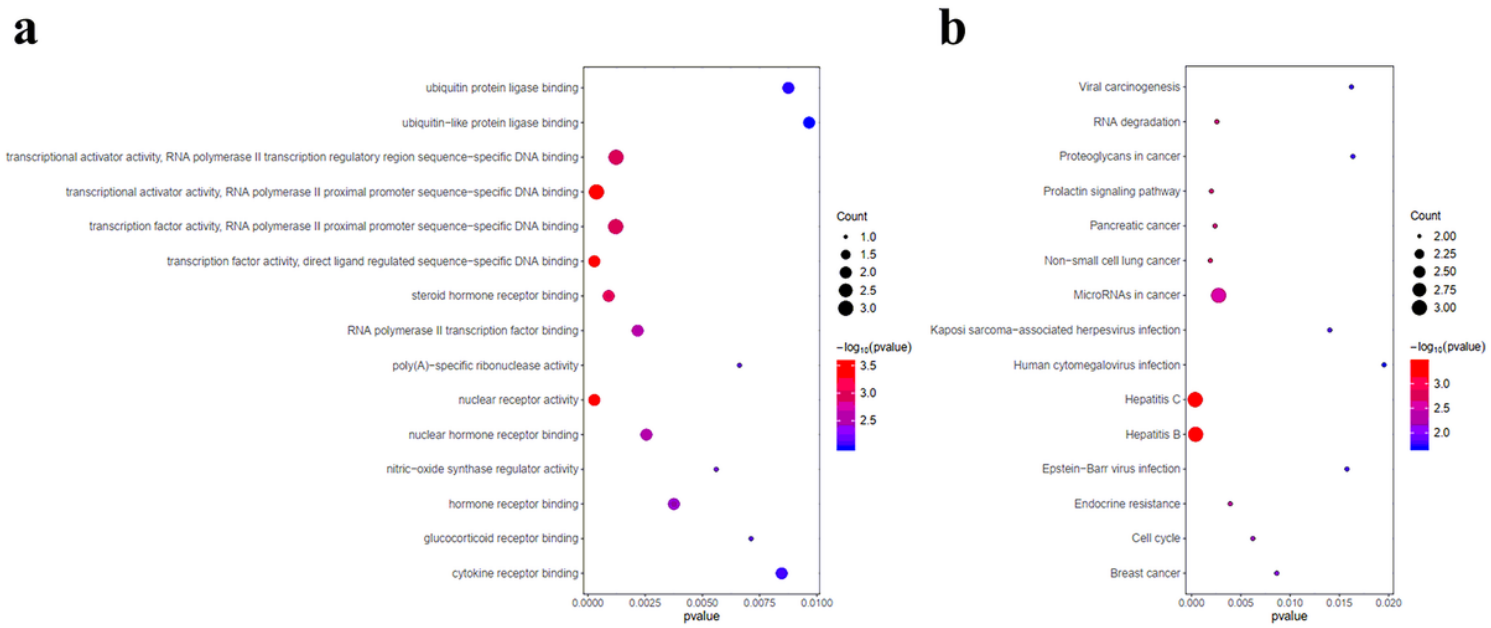

Figure 9

Functional analysis of 9 hub genes. a GO functional enrichment analysis of 9 hub genes. b KEGG pathway enrichment analysis of 9 hub genes.

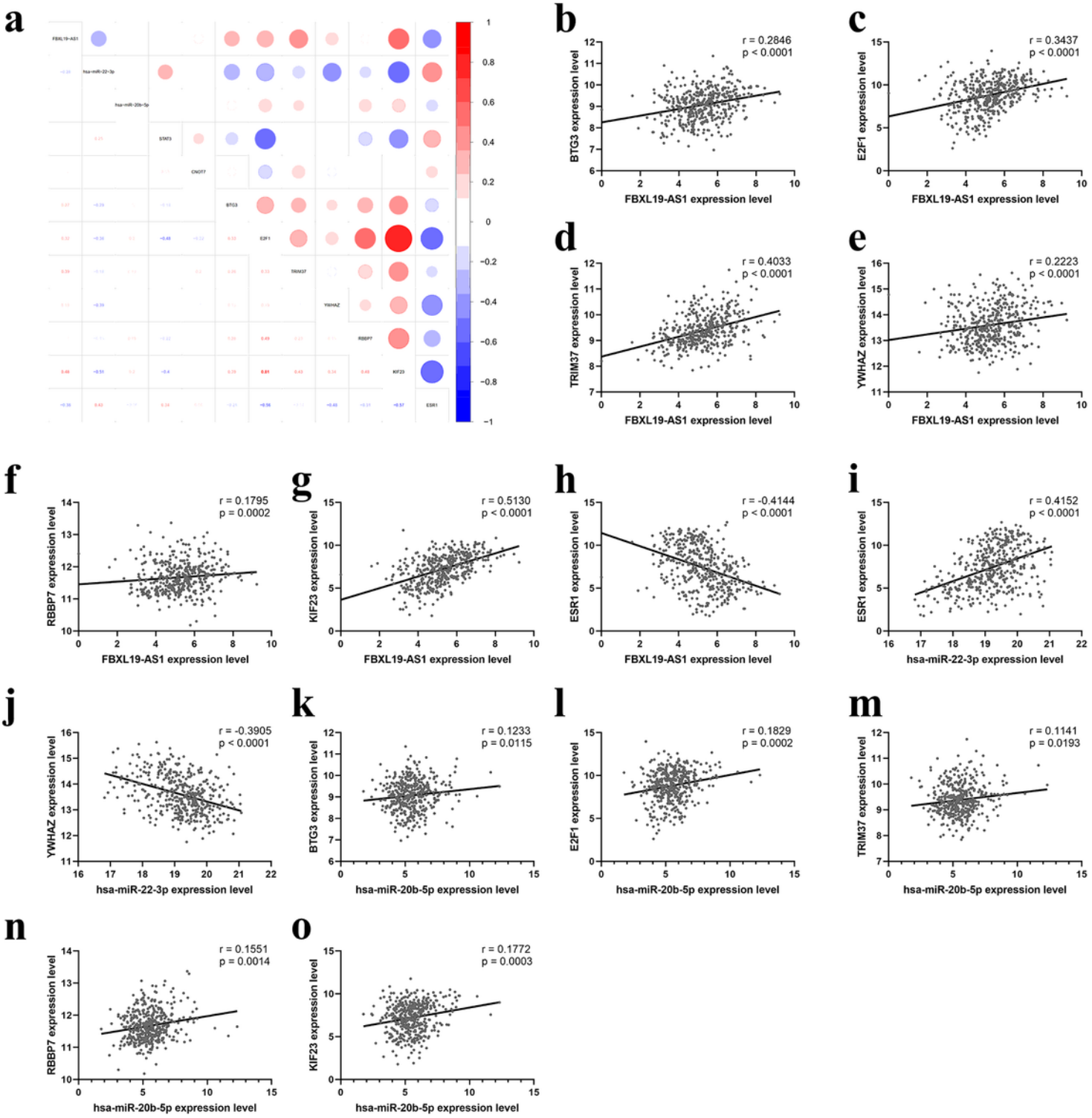

Figure 10

The correlation analysis of FBXL19-AS1, 2 miRNAs and 9 hub genes. a Correlation heatmap of the whole network. b-o The correlation analyses which were statistically significant.

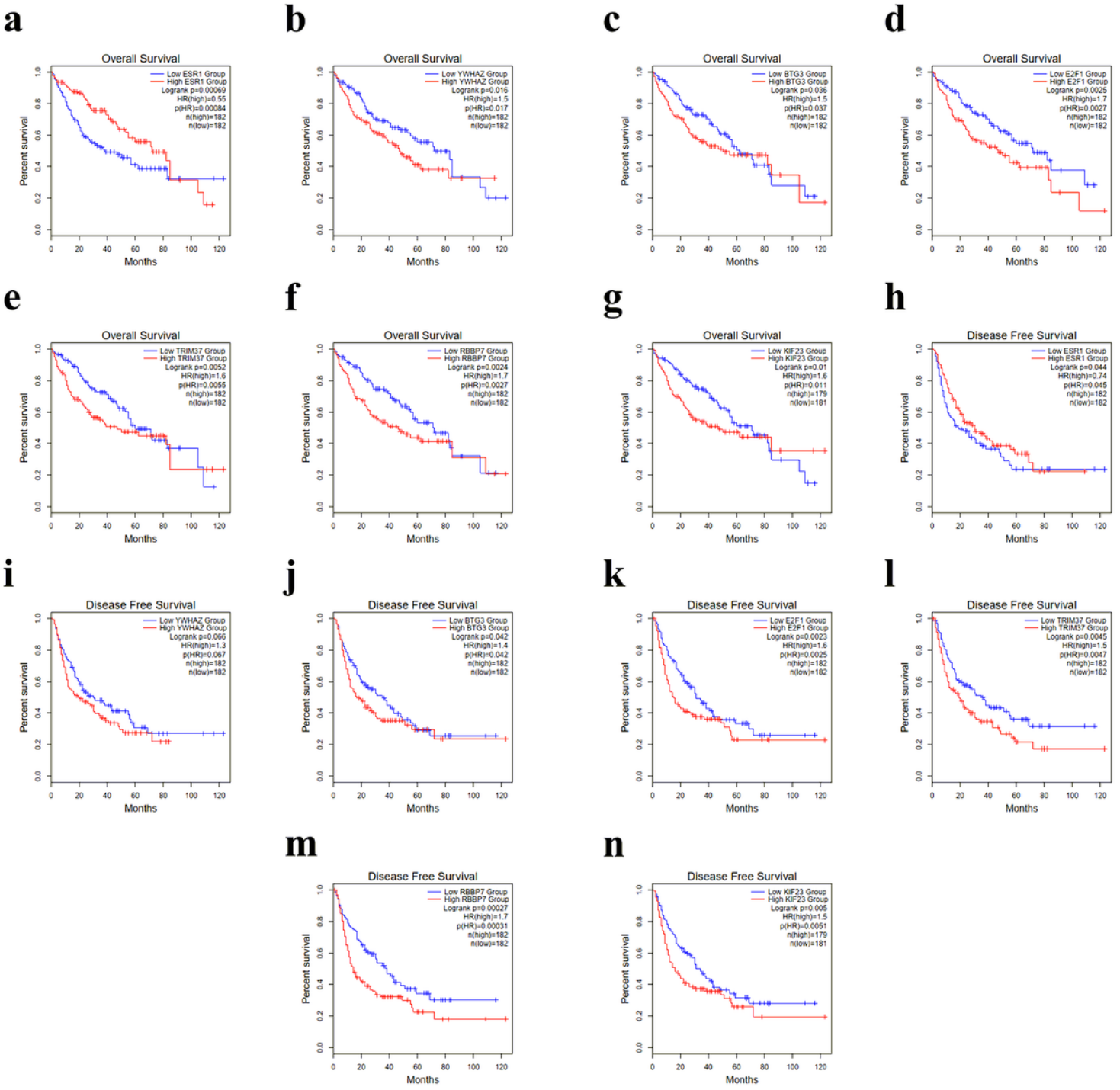

Figure 11

Overall survival and disease-free survival of 7 hub genes. a-g Overall survival of 7 hub genes. h-n Disease-free survival of 7 hub genes.

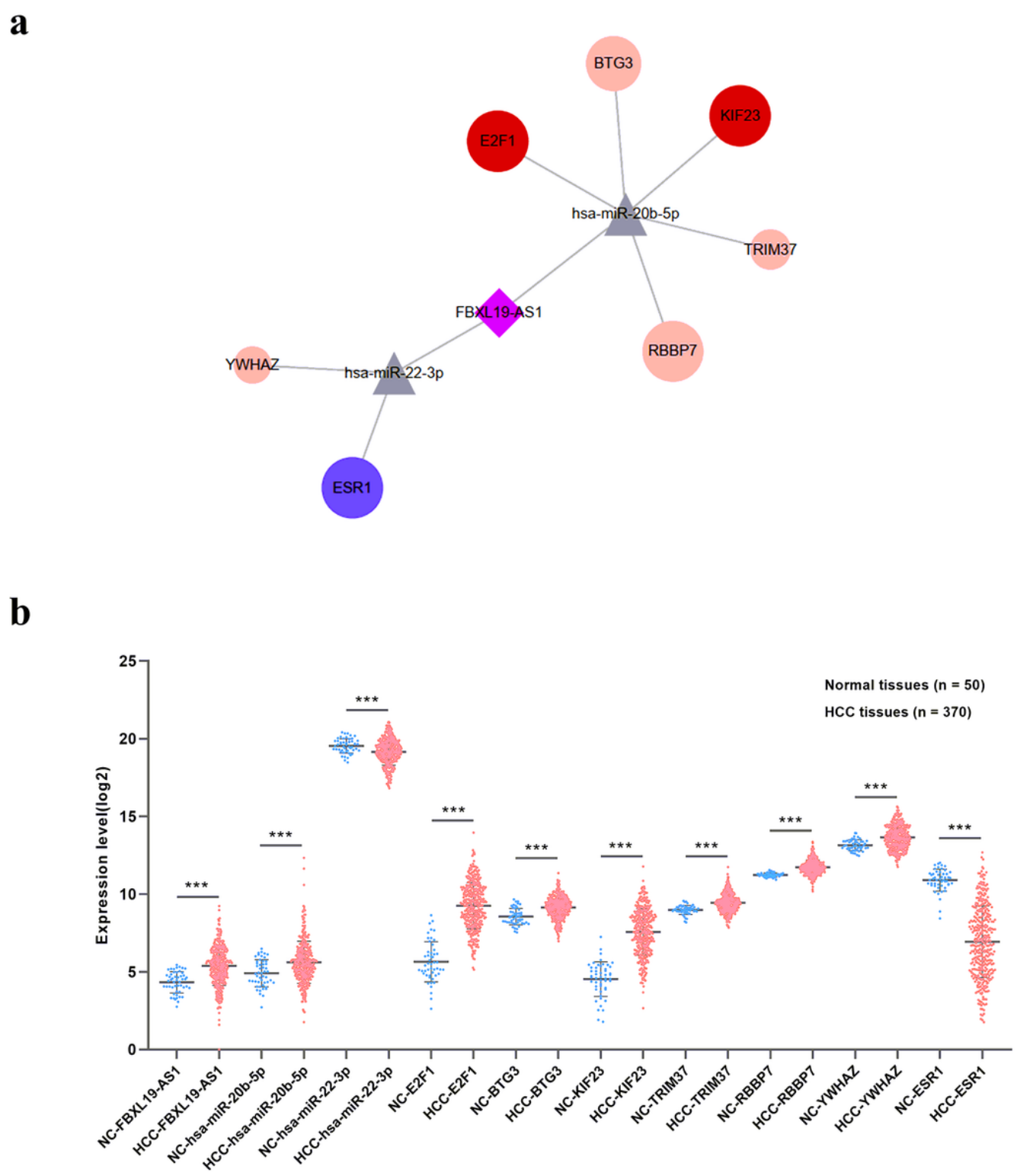

Figure 12

CeRNA network. a The network including 1 lncRNA (FBXL19-AS1), 2 miRNAs (has-miR-22-3p, has-miR-20b-5p) and 7 mRNAs (BTG3, E2F1, TRIM37, YWHAZ, RBBP7, KIF23, ESR1). b The expression levels of whole ceRNA network. * P < 0.05, ** P < 0.01 and ***P<0.001.

Supplementary Files

This is a list of supplementary files associated with this preprint. Click to download.

- Additionalfile8.pdf
- Additionalfile7.pdf
- Additionalfile6.pdf
- Additionalfile5.pdf
- Additionalfile4.pdf
- Additionalfile3.pdf
- Additionalfile2.pdf
- Additionalfile1.pdf